MODULAR MULTILEVEL CONVERTER WITH HARMONICS COMPENSATION FOR STATE-FEEDBACK CONTROLLER

A.U. Lawan[1], A.Abdulkarim[2], I.S Madugu[3], A.B. Kunya[2], G.S. Shehu[2],
[1]Department of Electrical Engineering, University of Nottingham, Malaysia.
[2]Department of Electrical Engineering, Zaria, Nigeria.
[3]Department of Electrical Engineering, Kano State University of Sci. & Tech. Wudil
[1]kecx4aua@nottingham.edu.my

Keywords: –
Controller.
Current reference,
Feed-forward,
Multilevel ,
state-feedback,

Article History: –
Received: January 2019.
Reviewed: April 2019
Accepted: May 2019
Published: September 2019

ABSTRACT

The voltage variations among the sub-module (SM) capacitors result in harmonics superimposed unto the circulating current. The conventional control of the SM voltages uses a closed-loop proportional Integral (PI) controller based on carrier shifted pulse width modulation (CSPWM). The PI-controller provides a dc reference circulating current for the control of the modular multilevel converter (MMC) measured circulating current. To decrease the influence of the voltage variation and improve the voltage control of the SM capacitors with harmonics elimination, this paper proposes a simple but an improved circulating current control within the MMC using a state-feedback controller. The proposed method employs state-feedback controller shaped by a linear quadratic regulator for a better reference tracking. The voltage disturbance in the PI-control loop is considered and disturbance rejection by feed forward compensation concepts is employed in the proposed scheme to produce an opposing compensation current to the circulating current reference. The feed forward current produced in the proposed method opposes and cancels the ac-harmonics due to the voltage disturbance/variations with simplicity and without the use of any additional filters or harmonic controllers such as resonant controllers. The MMC performance in the conventional method and proposed method is presented in a simulation. Finally, results from experiment are given to verify the simulation.

1. INTRODUCTION

Modular multilevel converter (MMC) technology is widely viewed as the recent configurations in power electronic industries. Their applications are possible due to multilevel controlled and balanced voltages that are shared among the switches [1-3]. There are many control schemes such as direct control, power synchronization, and direct-quadrature control, among others, applied to MMC [5]-[7],[8]. MMC applications for stability and control have been employed based on different modulation techniques for a different level of SM stacked cells [9-11], [12]. Balancing control of the stacked cells has been achieved using different methods [13-17], [18]. Control of capacitor voltages has been achieved using different approaches capacitors has an effect on the quality of the MMC outputs. The voltage variations that could arise due to poor voltage balancing control produce harmonics [22]. The voltage variation from within the MMC makes the circulating current to have ripple components [17].The use of the PI-controllers in the internal control of the MMC is one of the most common solutions to obtain a zero-static error in controlling the dc circulating current [23],[24]. However, PI-controllers have a little effect in suppressing the harmonic voltage ripple [25] unless high-gain high-order controllers, such as resonant controllers, are employed with the PI-controllers. Based on the integral feature of resonant controllers, the suppression of the low-order harmonic voltage could be achieved. This control is mostly achieved using second-order resonant controllers.

Another option to reducing the impact of harmonics in MMC is to add more filters such as in [26]. However, filters add delay and cost. A state-feedback controller instead of PI-controller can be employed for a current control such as in [27].The control in [27] was for an AC output current of a conventional two-level inverter

not in MMC applications such as the circulating current control. A good tracking of current was achieved. However, to target specific harmonics in the output current, resonant controllers had to be employed along with the state-feedback controller. Another option to suppressing the impact of disturbance is by employing a feed-forward concept, the typical example of feed forward disturbance strategy can be found in [28],[29] and in [30].

The paper is organized in the following way: Section II provides an overview of the MMC circulating current and capacitor voltage control based on CSPWM closed-loop control scheme. Section III introduces the circulating current control based on the proposed feed forward concept for a state-feedback circulating current controller. Simulation and experimental results of the proposed control method are presented in Section IV and V respectively, and the conclusion of the work is provided in Section VI.

2. CIRCULATING CURRENT AND CAPACITOR VOLTAGE CONTROLS IN THE CSPWM BASED MMCs

Fig. 1 depicts the three-phase MMC system. I_f and V_c are the MMC output current and voltage respectively. V_f is the reference voltage at the point of coupling (PCC) with respect to source voltage V_s. L_s is the source inductance and R_s is the source resistance. V_{dc} is the direct current (DC) link voltage. L_r is the arm inductance. R_r is the arm resistance. Applying Kirchhoff's principle on any leg/phase with respect to node *n*, the relationship between the per phase output current i_k, the lower and upper arm currents (i_{kp} and i_{kn}), and circulating current i_{cirk} are given by:

$$i_k = i_{kp} - i_{kn} \tag{1}$$

$$i_{cirk} = \frac{1}{2}\left(i_{kp} + i_{kn}\right) \tag{2}$$

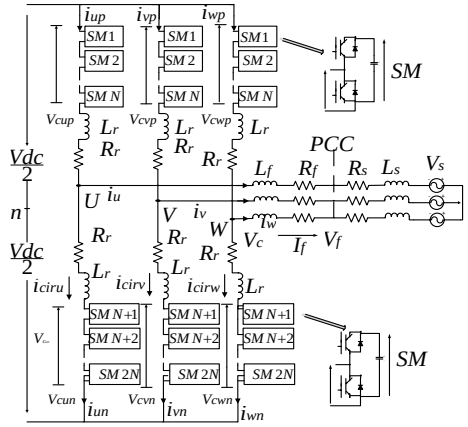

Fig. 1. *MMC in the three-phase configuration.*

The sub-script k represents any of the three-phases (u, v or w). Based on (1) and (2), the regulation of the circulating current i_{cirk} and the output voltage V_{ck} could be achieved by controlling i_{kp} and i_{kn} as in (1) and (2), and the upper arm voltage and lower arm voltages (V_{ckp} and V_{ckn}) given in (3) and (4) respectively. V_{ck} is given in (5).

$$V_{ckp} = \frac{1}{2}V_{dc} - V_{ck} \tag{3}$$

$$V_{ckn} = \frac{1}{2}V_{dc} + V_{ck} \tag{4}$$

$$V_{ck} = \frac{1}{2}V_{dc*}M\sin\left(\omega t\right) \tag{5}$$

Equation (5) gives the output voltage under ideal conditions when each voltage of the submodules (SM) capacitor is uniform and equivalent to V_{dc}/N. M is the modulation voltage and I_c is the peak output current. ω and φ are the angular frequency and load angle respectively. The per-phase controls which are the average capacitor voltage control, arm balancing control, and the individual control use (6)-(9) [25]. The symbols in Figs. 2 are as

$$\overline{\mathrm{V}}_{Ck} = \frac{1}{2}\left(\overline{\mathrm{V}}_{Ckp} + \overline{\mathrm{V}}_{Ckn}\right) \tag{6}$$

$$\overline{\mathrm{V}}_{Ckp} = \frac{1}{N}\sum_{i=1}^{N}\mathrm{V}_{Cki} \tag{7}$$

$$\overline{V}_{Ckn} = \frac{1}{N}\sum_{j=N+1}^{2N} V_{Ckj} \quad (8)$$

$$V_C^* = \frac{V_{dc}}{N} = V_{Ck}^* \quad (9)$$

$\overline{V}_{Ck}$ is the per-phase average capacitor voltage in the corresponding phase. $\overline{V}_{Ckn}$ and $\overline{V}_{Ckp}$ are the average capacitor voltage of the lower arm and upper arm of the corresponding leg respectively. N is the number of the SM in the upper and lower arm. V_{Cki} and V_{Ckj} are the voltages of the *i*th and *j*th SMs in the upper arm and lower arm respectively. V_{Ck}^* and i_{cirk}^* represent the reference voltage and reference circulating current in the corresponding leg respectively. Fig. 2(a) gives the averaging-capacitor voltage control diagram, this control pushes the averaging-capacitor voltage $\overline{V}_{Ck}$ of each phase leg to track the reference voltage V_{Ck}^*. When $V_{Ck}^* \geq \overline{V}_{Ck}$, i_{cirk}^* increases. This increase will impose the circulating current i_{cirk} to track its reference current i_{cirk}^* making $\overline{V}_{Ck}$ to track its reference voltage V_{Ck}^*. PI controllers can be employed in the tracking, and the output voltage command v_{cirk} from the averaging control can be produced for the CSPWM. The gains of the PI controllers which are K_1, K_2, K_3 and K_4 could be obtained based on internal mode control theory.

The individual-capacitor voltage balancing control pushes each SM capacitor voltage individually in every submodule to follow its voltage reference V_{Ck}^*, the individual balancing control is depicted in Fig. 2(b). The obtained voltage command for this modulation control is v_{kB}. When $V_{Ck}^* \geq V_{Ck(i,\,j)}$ the arm current is charging the SM capacitor, the polarity of the output current is positive. When it is reversed, the arm current gets the opposite polarity. The proportional controller with a gain K_3 could be employed.The control block for the arm balancing is shown in Fig. 2(c). This process lessens the discrepancies in voltages between the lower and upper arm voltages. The voltages, $\overline{V}_{Ckn}$ and $\overline{V}_{Ckp}$ are also named as the average voltages of the negative arm and positive arm respectively. The proportional controller K_6 could be employed. Similarly, the proportional controller K 4 could be employed [32]. Fig. 2(d) and (e) shows the proposed averaging control and the voltage commands for the CSPWM respectively. Note that the circulating current control based on Fig. 2(a) is usually insufficient in suppressing the circulating current harmonics [25]. Thus, voltage disturbance v kd will be introduced on the submodules, which injects harmonic current during normal operations [25]. Detail analysis of the voltage disturbance and its impact in the capacitor voltage control based on CSPWM can be found in [25]. In this paper, instead of using a repetitive controller or resonant controller as in [25], a feed forward compensation of the voltage disturbance is introduced to oppose the effect of the disturbance.In order to have better suppression of the harmonics in the circulating current at any specified frequency, controllers of high gain at the frequencies of the harmonics have to be used. A resonant controller has such feature [25], [34]. The circulating current PI controller when augmented with the resonant controller could be as follows: A resonant controller has such a feature [25], [34]. The circulating current PI controller with the resonant controller could be as

$$C_r(s) = K_{p\_i} + \frac{K_{i\_i}}{s} + \frac{2K_{rk}\omega_c s}{s^2 + 2\omega_c s + (h\omega_o)^2} \quad (10)$$

where K_{p_i} is the proportional gain and K_{i_i} as the integral gain. ω_c is the resonant controller bandwidth, ω_o is the fundamental frequency, K_{rk} is the h-order resonant controller gain, and h is any chosen order to be suppressed. The controller $C_r(s)$ has infinite gain at h-order harmonic frequency, therefore, it can eliminate the h-order disturbance of v_{kd}. Suppression of harmonics has been achieved based on the controller $C_r(s)$ of (10) in [34]. However, only second-order resonant controller is employed. However, only second-order resonant controller is employed. To achieve an improved suppression of harmonics,

additional high even order resonant controllers such as the fourth-order controllers have to be added.

3. THE PRPOSED VOLTAGE DISTURBANCE REJECTION WITH A FEEDBACK CONTROLLER

The voltage disturbance v_{kd} shown in Fig. 3 is reported to be the genesis of the harmonics in the arm of the MMC [25].The voltage disturbance results from the load current flowing through the submodule capacitors in the dc form.

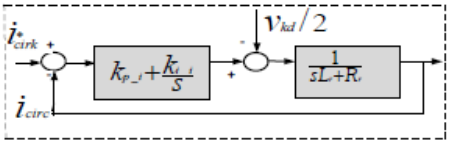

Fig. 3. Circulating current control using PI controller [25].

The variation results in the injection of the voltage disturbance onto the circulating current. This occurs at the twice of the fundamental current frequency. The excited circulating current consequently produces harmonics into the arm currents [25]. The general approaches to suppressing the harmonics are use of filters such as in [26], application of the high-order controllers such as the resonant controllers and repetitive controllers [25], and the injection of external second harmonic voltages [35-41]. In this paper instead of using additional filters, controllers or generation of a second harmonic voltage from an external source, gain. w is the resonant controller bandwidth, K is the h - the source of the harmonics which is the voltage disturbance is Identified from within the MMC measured quantities, then the order resonant controller gain, and h is any chosen order to be suppressed. The controller C (s) has an infinite gain at h–order harmonic frequency, therefore, it can eliminate the h-order disturbance of v. Suppression of harmonics has been current due to the voltage disturbance is extracted and feedback based on the feedforward method to counteract the ac-harmonic currents in the circulating current. The current extracted serves as opposing signal to the harmonic current, thus canceling their impact while the state-feedback controller regulates the circulating current. Taking in any phase-k, the variation could be explained by the stored energy in the number of SM capacitance C in the upper and lower arms are as follow in (11) [25],B ased on (7)-(8), the instantaneous active energy stored in the arms, and their relationship for a number of submodule capacitor C are as follows:

$$\left.\begin{aligned} W_{kp} &= \frac{1}{2N} C v_{Ckp}^2 \\ W_{kn} &= \frac{1}{2N} C v_{Ckn}^2 \end{aligned}\right\} \quad (11)$$

TABLE I
PARAMETERS OF THE CONTROL FOR SIMULATION AND EXPERIMENT

Symbol	Quantity	Value
K_1	Proportional outer DC capacitor voltage gain	0.1
K_2	Integral outer DC capacitor voltage gain	1.0
K_3	Proportional capacitor voltage gain	0.5
K_4	Proportional capacitor voltage gain	0.5
w_c	Resonant controller bandwidth	3.0
k_{r2}	Gain of the second order resonant control	300
k_{r4}	Gain of the fourth order resonant control	350

From (10) and (11), the voltage disturbance which contributes to the variation can be written in terms of the DC component i_{dc} and harmonic components i_n as given in (12) and (13).

$$\left.\begin{aligned} \Delta v_{Ckp} &= \frac{N}{2C}\int \left(1 - M\sin(\omega t)\right)\cdot\left(\frac{i_k}{2} + \frac{1}{3}i_{dc} + \sum_{n=1}^{\infty} i_n\right)dt \quad (12) \\ \Delta v_{Ckn} &= \frac{N}{2C}\int \left(1 + M\sin(\omega t)\right)\cdot\left(-\frac{i_k}{2} + \frac{1}{3}i_{dc} + \sum_{n=1}^{\infty} i_n\right)dt \quad (13) \end{aligned}\right\}$$

Δv_{Ckp} and Δv_{Ckn} are the voltage changes due to disturbances in the upper and lower arms of the MMC respectively. The circulating current is as

$$i_{cirk} = \frac{1}{3}i_{dc} + \sum_{n=1}^{\infty} i_n \quad (14)$$

where the harmonic components i_n are the nth order harmonics of the circulating current. Therefore,

the real output voltages of the upper and lower are as given in (15).

$$\left.\begin{aligned} v_{kp} &= \frac{1}{2}\left(1 - M\sin(\omega t)\right)\cdot\left(V_{dc} + \Delta v_{Ckp}\right) \\ v_{kn} &= \frac{1}{2}\left(1 + M\sin(\omega t)\right)\cdot\left(V_{dc} + \Delta v_{Ckn}\right) \end{aligned}\right\} \quad (15)$$

Then considering the voltage disturbance, the total output voltage of the phase would be given as follows:

$$v_{kp} + v_{kn} = V_{dc} + \frac{1}{2}\left(\Delta v_{Ckp} + \Delta v_{Ckn}\right) + \frac{1}{2}M\sin(\omega t)\cdot \quad (16)$$
$$\left(\Delta v_{Ckn} - \Delta v_{Ckp}\right) = V_{dc} + v_{kd}$$

v_{kd} in (16) is the voltage variation between the leg and the total submodule voltages when the system is under normal modulation and given as in (17).

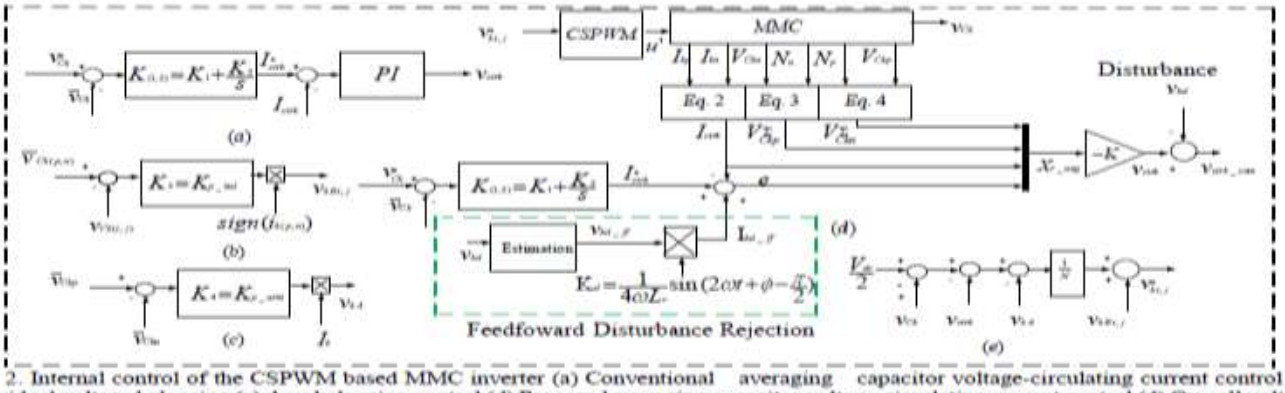

Fig. 2. Internal control of the CSPWM based MMC inverter (a) Conventional averaging capacitor voltage-circulating current control (b) Individual voltage balancing (c) Arm balancing control (d) Proposed averaging capacitor voltage-circulating current control (d) Overall voltage command generation.

It can be seen from (16) that can be obtained from the difference between the measured total capacitor voltages $v_{ckp,n}^{\Sigma}$,times the insertion indices *i.e.* $(v_{kp,n} = N_{p,n}v_{ckp,n}^{\Sigma})$ and the dc link value. The voltage disturbance v_{kd} of (15) that excites the circulating current at twice the fundamental frequency, thus, can be estimated as follows:

$$v_{kd} = \frac{1}{2}\left(\Delta v_{Ckp} + \Delta v_{Ckn}\right) + \frac{1}{2}M\sin(\omega t)\cdot\left(\Delta v_{Ckn} - \Delta v_{Ckp}\right) \quad (17)$$
$$\approx v_{kd\_2h}$$

Corresponding voltage and current disturbance are :

$$v_{kd} = v_{kd-2h} = v_{kd}.\sin(2\omega t + \phi) \quad (18)$$

And the current disturbance can be written as

$$i_{kd} = \int v_{kd-2h}\,dt = \frac{-v_{kd-2h}}{4\omega L_r}\sin(2\omega t + \phi - \frac{\pi}{2}) \quad (19)$$

$v_{kd-ff} = k.v_{kd-2h}$ can be used to present an estimated feed forward voltage to be used to generate the proposed feed forward current i_{kd-ff} that will augment the circulating current reference i_{cirk} as shown in Fig. 2. k is the estimation of the gains of the circulating current measuring devices.

4. IMPLEMENTATION AND SIMULATION RESULTS

The proposed control is done using MATLAB/Simulink. The modulation is validated using a nine-level MMC proto-type with four sub modules per arm. The modulation is carried out using carrier-shifted pulse width modulation scheme at 2KHZ. This means the overall switching frequency is 16KHZ.

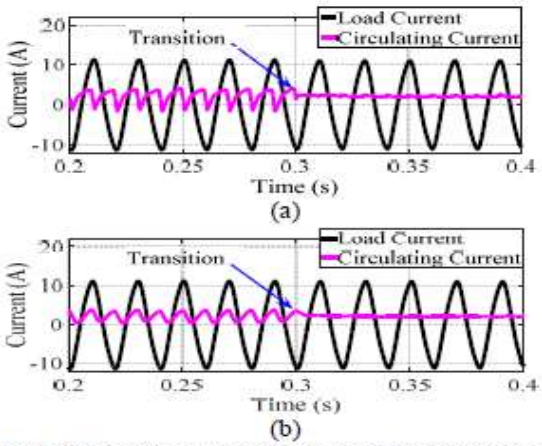

Fig. 4. Transition of load current and circulating current (a) from typical PI-control to proposed method (b) from PI+ R2th + R4th method to proposed method.

The gains of the PI controller have been chosen based on the pole-zero cancellation [37]. The control for the conventional method has been employed based on the PI- control scheme. The gain of the LQR is obtained using the Matlab based on the cost function; here, the optimal LQR parameters are obtained by applying standard Matlab functions lqrd [27].The inner circulating current control is carried out using the two methods: the conventional method based on Fig. 2(a) and the proposed state-feedback method based on Fig. 2(d).

To demonstrate the performance of the proposed method, 200VA MMC is tested under the simulation, a transition between the two reference currents, from typical PI-control to the proposed method is introduced as shown in Fig. 4(a). Another transition is depicted in Fig. 4(b), from the PI-control method with a resonant controller to proposed method with a resonant controller. The transitions are introduced at a time t=0.3sec.It can be seen that the harmonics in the circulating current are attenuated most under the proposed method with the resonant controller under PI-control with

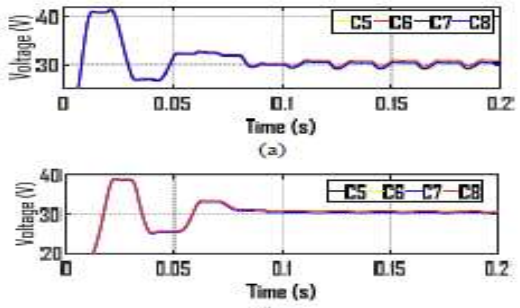

Fig. 5. Simulation of the capacitor voltages (a) conventional PI-control method (b) proposed method.

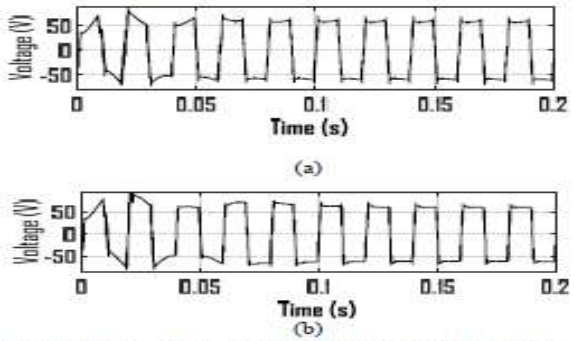

Fig. 6. Simulation waveforms of nine-level output AC voltage (a) conventional PI-control method (b) proposed method (state-feedback with feedforward disturbance rejection).

resonant controllers, and then under typical PI control method as the load current remains unaffected in all the methods. However, even without the resonant controller, it can be seen that the circulating current ripple has been suppressed.

Since the upper and lower arms are similar, Fig. 5 shows the capacitor voltages in the lower arm, it can be seen that the control based on the proposed method produced capacitor voltages with suppressed ripples and fewer overshoots. Fig .5 shows that the output voltage in the proposed method is less harmonic than in the conventional PI-control.

5. EXPERIMENTAL RESULTS

The experimental results that are shown in Fig. 7 are obtained from a small setup of a single phase of five-level MMC inverter with the parameters given in Table I. The control is implemented in the form of Simulink and executed using the DS1104 real-time controller. Channel 1 of Fig. 7(a) depicts the reference

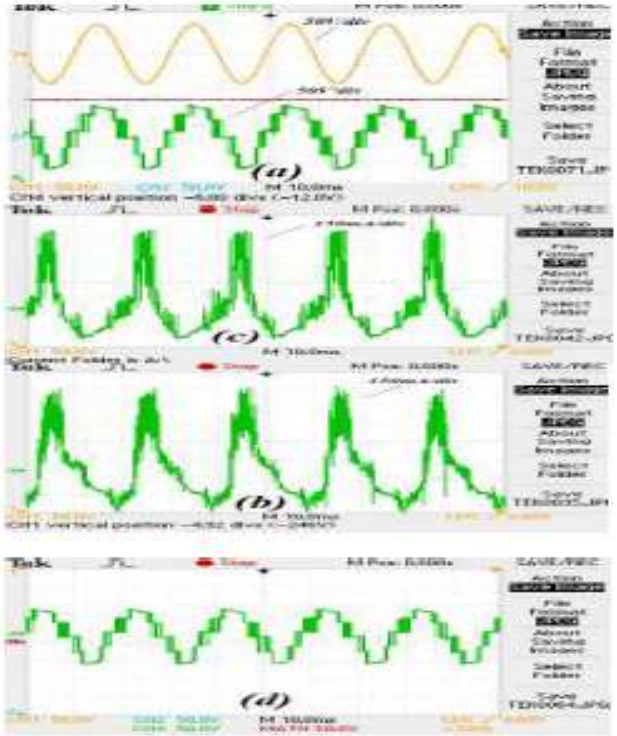

Fig. 7. Experimental waveform (a) channel 1: reference AC voltage channel 2: AC output voltage of 5-level single-phase MMC based on the proposed state-feedback method (b) circulating current based on the PI-control method (c) circulating current based on the proposed state-feedback with feedforward disturbance rejection.

AC voltage and channel 2 shows how the MMC output voltage tracks the reference voltage based on the proposed method. Figure 7(b) and (c) shows the circulating current obtained based on the PI-control method and the proposed state-feedback method respectively. The circulating current contains the dc current and ac-harmonics [38]. It can be seen that the state-feedback controlled current is less distorted than the conventional PI-control. Figure 7(d) shows the steady-state waveform of the five-level MMC inverter output voltage. Figs. 4, 5, 6, and 7 have illustrated how the proposed scheme produced an improved MMC performance.

6. CONCLUSION

This paper presents a concept of average capacitor voltage and circulating current control of MMC based inverter with a state-feedback controller. The outer-loop average capacitor voltage control of the MMC provides the reference circulating current for both the state-feedback controller and the conventional PI-controller circulating current control can usually be achieved by the use of PI-controllers with controllers such as the resonant controllers.

This paper illustrates that a similar control can be achieved by counteracting the voltage disturbance within the leg of the MMC. This can be achieved by providing an opposing feed forward voltage signal to suppress the impact of the voltage disturbance in generating voltage ripple and harmonics without the use of harmonic filters. The proposed controller is compared with the conventional PI-controller for circulating current harmonics elimination. The obtained simulation results show how the proposed control scheme achieved an improved circulating current control, fewer harmonics due to reduced capacitor voltage variations and good AC output voltage. The results from the two different control schemes are presented. The experimental steady-state results have validated the proposed control.

REFERENCES

[1] P. Rao, M.L. Crow, Z. Yang, STATCOM control for power system voltage control applications, IEEE Trans. Power Deliv. 15 (2000) 1311-1317.

[2] K. Ilango, A. Bhargav, A. Trivikram, P.S. Kavya, G. Mounika, M.G. Nair, Power Quality Improvement using STATCOM with Renewable Energy Sources, Power Electron. (IICPE), 2012 IEEE 5th India Int. Conf. (2012) 1-6,.

[3] D.M. Reddy, Dynamic Performance of Power Quality Improvement Using Multilevel DSTATCOM with DG Application, (2014).

[4] A.U. Lawan, M. Student, H. Abbas, J.G.K.S. M, A.A. Karim, Dynamic performance of Improvement of MMC Inverter with STATCOM Capability interfacing PMSG Wind Turbines with Grid, 2015 IEEE Conf. Energy Convers. (2015) 492-497.

[5] A.U. Lawan, M. Mustapha, I. Abubakar, M. Mustapha, I. Abubakar, Reactive current control of STATCOM based MMC Inverter for Wind Turbines connected to Grid, 2015 IEEE Student Conf. Res. Dev. (2015) 26-31.

[6] L. Liu, H. Li, Y. Xue, W. Liu, Reactive power compensation and optimization strategy for grid-interactive cascaded photovoltaic systems, IEEE Trans. Power Electron. 30 (2015) 188-202.

[7] H. Wang, F. Blaabjerg, A. East, Reactive Power Compensation Capability of a STATCOM based on Two Types of Modular Multilevel Cascade Converters for Offshore Wind Application, (2017) 326-331.

[8] F. Chouaf, S. Saad, A New Structure of the Nine Level Inverter Used as Active Power Filter with a Reduced Number of Swiches, 9 (2018) 198-209..

[9] A.U. Lawan, N. Magaji, H. Musa, A STATCOM Controller for Small Signal Stability using Polynomial Algorithms in a Horizontal Axis Wind Farm Power System, 2013 IEEE Energytech USA. (2013) 1-5.

[10] N. Magaji, A.U. Lawan, A.D.O. Dan-isa, M.W. Mustafa, Design A STATCOM supplementary Controller for Stability Studies using various state

feedback algorithm, Recent Res. Circuits Syst. (2012) 38-43.
[11] A.U. Lawan, State Feedback Approaches for Designing A Statcom Supplementary Controller for Oscillations Damping, Int. J. Eng. Sci. 3 (2014) 27-37.
[12] T. Porselvi, K. Deepa, R. Muthu, FPGA Based Selective Harmonic Elimination Technique for Multilevel Inverter, 9 (2018) 166-173.
[13] Y. Zhang, G.P. Adam, T.C. Lim, S.J. Finney, B.W. Williams, Analysis of modular multilevel converter capacitor voltage balancing based on phase voltage redundant states, IET Power Electron. 5 (2012) 726.
[14] M.M.C. Merlin, T.C. Green, Cell capacitor sizing in multilevel converters: cases of the modular multilevel converter and alternate arm converter, IET Power Electron. 8 (2015) 350-360.
[15] L. Norum, H. Nademi, Analytical circuit oriented modelling and performance assessment of modular multilevel converter, IET Power Electron. 8 (2015) 1625-1635.
.
[16] S. Liu, J. Jiang, Y. Wan, Generalised analytical methods and current-energy control design for modular multilevel cascade converter, IET Power Electron. 6 (2013) 495-504.
[17] R. Lizana, S. Member, M.A. Perez, S. Member, D. Arancibia, J.R. Espinoza, J. Rodriguez, Decoupled Current Model and Control of Modular Multilevel Converters, IEEE Trans. Ind. Electron. 62 (2015) 5382-5392.
[18] T. Poompavai, P.V. Priya, Comparative analysis of modified multilevel DC link inverter with conventional cascaded multilevel inverter fed induction motor drive, Energy Procedia. 117 (2017) 336-344. doi:10.1016/j.egypro.2017.05.140.
[19] K. Shen, J. Wang, D. Zhao, M. Ban, Y. Ji, X. Cai, Investigation of capacitor voltage regulation in modular multilevel converters with staircase modulation, J. Power Electron. 14 (2014) 282-291.
[20] B. Li, D. Xu, D. Xu, Circulating current harmonics suppression for modular multilevel converters based on repetitive control, J. Power Electron. 14 (2014) 1100-1108.
[21] H. Peng, Y. Wang, K. Wang, Y. Deng, X. He, R. Zhao, A Simple Capacitor Voltage Balancing Method with a Fundamental Sorting Frequency for Modular Multilevel Converters, 14 (2014) 1109-1118.
[22] M. Miranbeigi, Y. Neyshabouri, H. Iman-Eini, State feedbackcontrol strategy and voltage balancing scheme for a transformer-less STATic synchronous COMpensator based on cascaded H-bridge converter, IET Power Electron. 8 (2015)
[23] Y. Zhang, G.P. Adam, T.-C. Lim, S.J. Finney, B.W. Williams, Mathematical Analysis and Experiment Validation of Modular Multilevel Converters, J. Power Electron. 12 (2012) 33-39.
[24] N. Quach, S.H. Chae, S. Song, E. Kim, Frequency and Voltage Control Strategies of the Jeju Island Power System Based on MMC-HVDC Systems, 18 (2018) 204-211.
[25] M. Zhang, L. Huang, W. Yao, Z. Lu, Circulating harmonic current elimination of a CPS-PWM-based modular multilevel converter with a plug-in repetitive controller, IEEE Trans. Power Electron.
29 (2014) 2083-2097.
[26] V.G. Agelidis, J. Pou, S. Ceballos, R. Darus, Konstantin, Controllers for eliminating the ac components in circulating current of modular multilevel conv. IET Power Electron. 9 (2016) 1-8.
[27] B. Ufnalski, A. Kaszewski, L.M. Grzesiak, Particle Swarm Optimization of the Multioscillatory LQR for a Three-Phase Four-Wire Voltage-Source Inverter With Output Filter, IEEE Trans. Ind. Electron. 62 (2015) 484-493.
[28] Y. Bao, L.Y. Wang, C. Wang, J. Jiang, C. Jiang, C. Duan, Adaptive Feedforward Compensation for Voltage Source Disturbance Rejection in DC-DC Converters, IEEE Trans. Control Syst. Technol. 26 (2018) 344-351.
[29] A. Kaszewski, B. Ufnalski, L.M. Grzesiak, An LQ controller with disturbance feedforward for

the 3-phase 4-leg true sine wave inverter, Proc. IEEE Int. Conf. Ind. Technol. 0 (2013) 1924-1930.
[30] C. Edwards, P.P. Menon, N.M. Gomes Paulino, Observer-based controller design with disturbance feedforward framework for formation control of satellites, IET Control Theory Appl. 9 (2015) 1285-1293.
[31] J.I.Y. Ota, Y. Shibano, H. Akagi, A Phase-Shifted PWM D-STATCOM Using a Modular Multilevel Cascade Converter (SSBC)— Part II : Zero-Voltage-Ride-Through Capability, IEEE Trans. Ind. Appl. 51 (2015) 289-296.
[32] M. Hagiwara, R. Maeda, H. Akagi, Control and analysis of the modular multilevel cascade converter based on double-star chopper-cells (MMCC-DSCC), IEEE Trans. Power Electron. 26 (2011) 1649-1658.
[33] L.K. Haw, M.S.A. Dahidah, S. Member, H.A.F. Almurib, S. Member, A New Reactive Current Reference Algorithmfor the STATCOM System Based on Cascaded Multilevel Inverters, IEEE Trans. POWER Electron. 30 (2015) 3577-3588.
[34] Q. Tu, Z. Xu, L. Xu, Reduced Switching-frequency modulation and circulating current suppression for modular multilevel converters, IEEE Trans. Power Deliv. 26 (2011) 2009-2017.
[35] A. U. Lawan, Babani, A. Abdulkarim, G. S. Shehu, Y. Jibril, I. S. Madugu, ―Power Compensation for Vector-based Current Control of a Modular Multilevel Converter (MMC) based STATCOM‖ International Journal of Power Electronics and Drives (IJPEDS) vol.10, no. 4, pp. 71~85, 2019).
[36] A. U. Lawan, Haider A.F. Almurib, Jeen G. Khor ―Modular Multilevel Converter (MMC) based STATCOM with Vector Control and Virtual Impedance Voltage Compensations‖ International Journal of Power Electronics and Drives (IJPEDS), vol. 10, no. 4, pp. 51~70, 2019.
[37] A. U. Lawan, H. Abbas, J. G Khor , ― Enhanced decoupled Current Control with Voltage Compensation for Modular Multilevel Converter (MMC) based STATCOM‖ International journal of Power Electronics and Drives (IJPEDS) vol.10, no.3, pp.1483-1499, 2019.
[38] Ibrahim S. Madugu, B. J. Olufeagba, Yinusa A. Adediran, F. Abdulkadir, A. Abdulkarim James. U. Inaku, A. U. Lawan (2019) "A novel model for solar radiation prediction" TELKOMNIKA, 17(6), pp.3110-3119
[39] Ibrahim S. Madugu, B. J. Olufeagba, Yinusa A. Adediran, A. Abdulkarim, F. Abdulkadir, James. U. Inaku, Olalekan Ogunbiyi, O. Ibrahim2, A. U. Lawan, and Mubarak A. Afolayan " Arma Model for Prediction of Solar Radiation in Kano-Nigeria " Zaria Journal of Electrical Engineering Technology, Department of Electrical Engineering, Ahmadu Bello University, Zaria – Nigeria. 8(1),pp 1-8. (2019).
[40] SZ Hassan, H Li, T Kamal, A Arsalan, AU Lawan "Performance of grid-integrated Wind/ Microturbine/battery Hybrid renewable power system" Power and Energy conversion (PECon), IEEE International Conference on power and energy conversion Malaysia, 78-83, (2016)
[41] A.U. Lawan, H. Abbas, J. G Khor, S. Babani. "Circulating current control of a Modular Multilevel converter (MMC) with State Feedback Controller and Harmonic Suppression" ESRAS-ITEC/EUROPE IEEE Conference Nottingham UK. 1-8. (2018)